Generalization of the Lyddane-Sachs-Teller Relation to Disordered Dielectrics

T. W. Noh[(a)] and A. J. Sievers
Laboratory of Atomic and Solid State Physics and Materials Science Center, Cornell University, Ithaca, New York 14853
(Received 1 June 1989)

Sum rules and causality are used to obtain a general relation connecting the dynamic and static properties of any dielectric system which supports polarization waves. The Lyddane-Sachs-Teller relation appears as a special limiting case. Inhomogeneous media provide illustrative examples.

PACS numbers: 42.20.Dd, 63.50.+x, 77.80.−e

The Lyddane-Sachs-Teller (LST) relation[1] remains a corner stone in the understanding of displacive ferroelectricity. Fröhlich[2] and Cochran[3] first recognized the connection between the static and dynamic properties of ferroelectrics because the LST relation for a simple homogeneous dielectric,

$$\epsilon_0/\epsilon_\infty = \omega_l^2/\omega_t^2 , \tag{1}$$

provided a connection between the transverse and longitudinal frequencies, ω_t and ω_l, and the dc and optical dielectric constants, ϵ_0 and ϵ_∞, in the dielectric response function. Equation (1) has been generalized to cubic crystals with more than two atoms per unit cell[3] and also to include the case of damping.[4] In addition, Barker[5] found that Eq. (1) could be obtained from a causality argument if the response approximated a δ-function mode at ω_t. All of these extensions treat single crystals.

With sum-rule and causality arguments we show that for any nonconductor the ratio of the static and high-frequency dielectric constants equals the ratio of second moments of the longitudinal and transverse loss. By simulation this general relation is shown to describe exactly the connection between the dynamic and static properties of inhomogeneous media in the long-wavelength limit for two distinct topologies.

Consider a nonmagnetic linear isotropic dielectric system which is described by the dielectric function $\epsilon(\omega) = \mathrm{Re}\epsilon(\omega) + i\,\mathrm{Im}\epsilon(\omega)$. Two kinds of response functions occur since there are two kinds of vector polarization fields, solenoidal and irrotational, in the system. For a solenoidal response the loss function is $\mathrm{Im}[\epsilon(\omega)/\epsilon_\infty]$ while the corresponding irrotational loss function is $\mathrm{Im}[-\epsilon_\infty/\epsilon(\omega)]$.

One way to identify characteristic frequencies of this arbitrary system is using a moment representation.[6] With the LST relation in mind, we define a weighted second moment of the solenoidal and irrotational loss peaks as

$$\langle\omega^2\rangle_t \equiv \left[\int_0^\infty \frac{dx}{x} x^2 \mathrm{Im}\left(\frac{\epsilon(x)}{\epsilon_\infty}\right)\right] \times \left[\int_0^\infty \frac{dx}{x} \mathrm{Im}\left(\frac{\epsilon(x)}{\epsilon_\infty}\right)\right]^{-1} \tag{2}$$

and

$$\langle\omega^2\rangle_l \equiv \left[\int_0^\infty \frac{dx}{x} x^2 \mathrm{Im}\left(\frac{-\epsilon_\infty}{\epsilon(x)}\right)\right] \times \left[\int_0^\infty \frac{dx}{x} \mathrm{Im}\left(\frac{-\epsilon_\infty}{\epsilon(x)}\right)\right]^{-1} \tag{3}$$

using an obvious notation.

Next we make use of a general sum-rule result that[7,8]

$$\int_0^\infty dx\, x\, \mathrm{Im}\left[\frac{-\epsilon_\infty}{\epsilon(x)}\right] = \int_0^\infty dx\, x\, \mathrm{Im}\left[\frac{\epsilon(x)}{\epsilon_\infty}\right] . \tag{4}$$

Each of the integrals involved is an "f-sum rule" which can be obtained from a Kramers-Kronig relation plus the requirement that in the high-frequency limit the response is free-particle-like. Therefore, the numerator in Eq. (3) is equal to the numerator in Eq. (2) and the ratio of the two equations simplifies to

$$\frac{\langle\omega^2\rangle_l}{\langle\omega^2\rangle_t} = \frac{\int_0^\infty (dx/x)\mathrm{Im}[\epsilon(x)/\epsilon_\infty]}{\int_0^\infty (dx/x)\mathrm{Im}[-\epsilon_\infty/\epsilon(x)]} . \tag{5}$$

A Kramers-Kronig integral connecting the real and imaginary parts of the solenoidal response function is[9]

$$\frac{2}{\pi}\int_0^\infty dx \frac{x\,\mathrm{Im}[\epsilon(x)/\epsilon_\infty]}{x^2-\omega^2} = \mathrm{Re}\left[\frac{\epsilon(\omega)}{\epsilon_\infty}\right] - 1 , \tag{6}$$

which when evaluated at $\omega = 0$ reduces to

$$\frac{2}{\pi}\int_0^\infty \frac{dx}{x} \mathrm{Im}\left[\frac{\epsilon(x)}{\epsilon_\infty}\right] = \frac{\epsilon_0}{\epsilon_\infty} - 1 . \tag{7}$$

In a similar manner one can evaluate at $\omega = 0$ the corresponding Kramers-Kronig relation for the irrotational response, and find

$$\frac{2}{\pi}\int_0^\infty \frac{dx}{x} \mathrm{Im}\left[\frac{-\epsilon_\infty}{\epsilon(x)}\right] = 1 - \frac{\epsilon_\infty}{\epsilon_0} . \tag{8}$$

Since Eqs. (7) and (8) are the numerator and denominator of Eq. (5), then

$$\frac{\langle\omega^2\rangle_l}{\langle\omega^2\rangle_t} = \frac{\epsilon_0/\epsilon_\infty - 1}{1 - \epsilon_\infty/\epsilon_0} = \frac{\epsilon_0}{\epsilon_\infty} , \tag{9}$$

which is the desired result. *For a general system, the ratio of a particular class of second moments is equal to the ratio of the low- and high-frequency dielectric constants.*

Let's first apply Eq. (9) to the single-crystal case. For a cubic crystal with a single ir-active vibrational mode the appropriate dielectric function is

$$\frac{\epsilon(\omega)}{\epsilon_\infty} = \frac{\omega_l^2 - \omega^2 - i\gamma\omega}{\omega_t^2 - \omega^2 - i\gamma\omega}. \tag{10}$$

Substituting this expression into Eqs. (7) and (8) gives values for the integrals of ω_p^2/ω_t^2 and ω_p^2/ω_l^2, respectively, where $\omega_p^2 = \omega_l^2 - \omega_t^2$; hence the "crystalline" LST relation is recovered.

To illustrate the generality of Eq. (9), we consider a vibrational model in which both the dc dielectric constant and weighted loss spectra can be calculated but one which does not necessarily produce the single-crystal spectrum described by Eq. (10). The long-wavelength response of inhomogeneous dielectric media are ideal for this purpose. Depending on the topology of the structure, two different mean-field methods are available to describe both the dc and optical properties of composites, the Maxwell-Garnett (MG) and the Bruggeman [effective-medium-approximation (EMA)] models.[10]

We treat the vibrational response of a two-component composite, one component inert ($\epsilon_a = \epsilon_{a\infty} = 10$) and the other obeying Eq. (10) (parameter values: $\omega_t = 5$ cm^{-1}, $\omega_t/\gamma = 1$, $\omega_l/\omega_t = 100$, and $\epsilon_{b\infty} = \epsilon_{a\infty}/2 = 5$). These values are reasonable for a particle mixture of a displacive ferroelectric, at a temperature just above the phase transition value, and Si (the inert material) of volume fill fraction f.

Figure 1 presents, for each composite-medium model, the spectral density of the solenoidal strength as a function of the volume fill fraction. The EMA model, Fig. 1(a), shows that with increasing f the spectral density is shifted up in frequency into a broad impurity band. The pole at ω_t disappears for $f > \frac{2}{3}$.[8] The change in the spectrum for the MG model with increasing f is very different [Fig. 1(b)] with a new, sharp spectral feature, a void resonance, produced at larger frequencies. Considered together both calculations demonstrate that the spectral weight shifts from low to high frequencies with increasing f.

Figure 2 shows a similar development in the spectral density of the irrotational strength with increasing f but now the shift is to lower frequencies. The EMA [Fig. 2(a)] generates an asymmetric distribution with the pole at ω_l disappearing for $f > \frac{1}{3}$.[8] For the MG model [Fig. 2(b)] the pole remains intact with increasing f but a new spectral feature appears at lower frequencies.

For the EMA model we calculate $\epsilon_0/\epsilon_\infty$ and also evaluate Eqs. (2) and (3) as a function of f. The root-mean-square moment frequencies are presented in Fig. 3(a). Note that $(\langle\omega^2\rangle_t)^{1/2}$ changes rapidly while $(\langle\omega^2\rangle_l)^{1/2}$ is nearly independent of f so that both frequencies approach the isolated-sphere resonance frequency of the near-ferroelectric material at large f. In Fig. 3(b) the solid curve gives the calculated dependence of $\epsilon_0/\epsilon_\infty$ and the circles, that of $\langle\omega^2\rangle_l/\langle\omega^2\rangle_t$. The ratio calculations for the MG model are also shown here. Be-

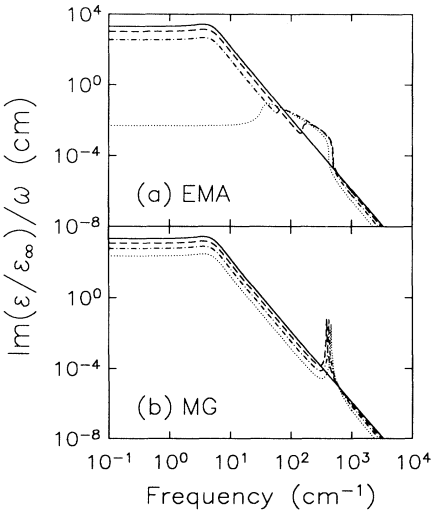

FIG. 1. Spectral density of the solenoidal strength for a composite with one ir-active component. (a) Calculated with the EMA model. (b) Calculated with the MG model, inert material embedded in the near ferroelectric. Volume fill fraction of the inert material is f. Solid curve: $f = 0$, near-ferroelectric medium described in the text; dashed curve: $f = 0.25$; dot-dashed curve: $f = 0.5$; dotted curve: $f = 0.75$.

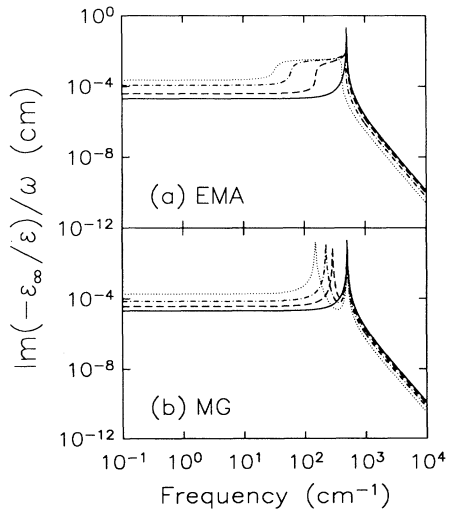

FIG. 2. Spectral density of the irrotational strength for a composite with one ir-active component. Same parameters as described in Fig. 1.

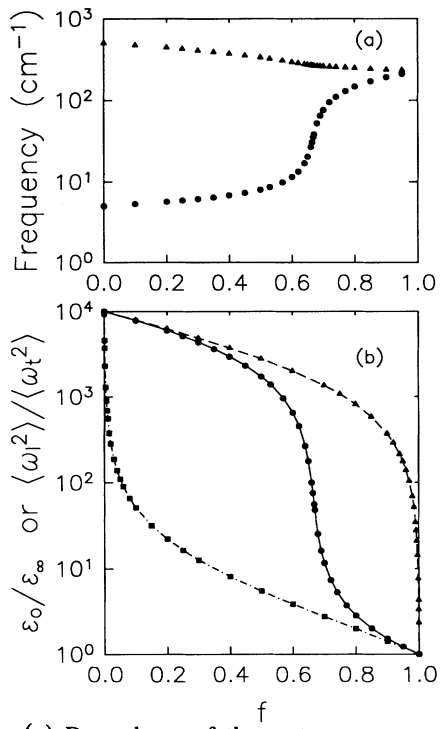

FIG. 3. (a) Dependence of the root-mean-square frequencies on f for the EMA model. Triangles: $(\langle\omega^2\rangle_l)^{1/2}$. Circles: $(\langle\omega^2\rangle_t)^{1/2}$. (b) Dependence of the ratio of the second moments and of the dc dielectric constant on f. EMA calculations: solid curve, $\epsilon_0/\epsilon_\infty$; circles, $\langle\omega^2\rangle_l/\langle\omega^2\rangle_t$. MG calculations: inert material embedded in the near ferroelectric: dashed curve, $\epsilon_0/\epsilon_\infty$; triangles, $\langle\omega^2\rangle_l/\langle\omega^2\rangle_t$. The dot-dashed line and squares are similar calculations but for the near ferroelectric embedded in the inert material.

cause the two components are treated in an asymmetric way in this model, there are two possible arrangements, one for medium a surrounded by b and visa versa. Both possibilities are presented in Fig. 3(b). The broken curves correspond to $\epsilon_0/\epsilon_\infty$ and the squares and triangles to the values of $\langle\omega^2\rangle_l/\langle\omega^2\rangle_t$. Although the EMA and MG models distribute the spectral weight of the solenoidal and irrotational response functions in different ways, the second-moment expression, Eq. (9), holds independent of these topological details.

The recent measurements of the reststrahlen band of diamond:ZnS composites[11] provide one experimental test of Eqs. (2), (3), and (9). As the diamond fill fraction f increases to 33%, the pole frequency and zero crossing of the vibrational spectrum remain essentially unchanged, yet for frequencies below this TO mode the reflectivity (hence ϵ_0) decreases. These results are not consistent with Eq. (1); however, when the moments [Eqs. (2) and (3)] are calculated from the published spectral data[11] good agreement is found with Eq. (9) at each f value.

The published optical constants[12] for single-crystal Si over the broad electronic interband frequency region permit another more extensive experimental test. By numerical integration from 107 to 0.161 eV, we obtain $\langle\omega^2\rangle_t = 27.033$ (eV)^2 and $\langle\omega^2\rangle_l = 310.777$ (eV)^2 so that $\langle\omega^2\rangle_l/\langle\omega^2\rangle_t = 11.50$. The value of this ratio is within 1% of that obtained from the ratio of the dielectric constants at the two limiting frequencies, $\epsilon_0/\epsilon_\infty = 11.715/1.0134 = 11.56$, in accord with Eq. (9). Hence, the sum-rule arguments supported by the illustrative calculations with composites together with these Si interband numerical results demonstrate that Eq. (9), the generalized LST relation, characterizes the long-wave displacement-current response of electronic or vibrational degrees of freedom in an ordered or disordered dielectric medium.

We thank A. S. Barker, R. P. Devaty, J. A. Krumhansl, and J. B. Page for helpful discussions. This work was supported by NSF Contract No. DMR-87-14600, ONR Contract No. N00014-87-K-0527, and ARO Contract No. DAAL03-86-K-01103.

[a]Present address: Department of Physics, Seoul National University, Seoul 151-742, Korea.

[1]R. H. Lyddane, R. G. Sachs, and E. Teller, Phys. Rev. **59**, 673 (1941).

[2]H. Fröhlich, *Theory of Dielectrics* (Clarendon, Oxford, 1949).

[3]W. Cochran, Phys. Rev. Lett. **3**, 521 (1959); Adv. Phys. **9**, 387 (1960).

[4]A. S. Barker, Jr., Phys. Rev. **136**, A1290 (1964).

[5]A. S. Barker, Jr., Phys. Rev. B **12**, 4071 (1975).

[6]This approach is to be contrasted with that of Ref. 5 where a number of modes are defined, each represented by a complex frequency.

[7]M. Altarelli, D. L. Dexter, H. M. Nussenzveig, and D. Y. Smith, Phys. Rev. B **6**, 4502 (1972).

[8]D. Stroud, Phys. Rev. B **19**, 1783 (1979).

[9]F. Stern, in *Solid State Physics: Advances in Research and Applications,* edited by H. Ehrenreich, F. Seitz, and D. Turnbull (Academic, New York, 1963), Vol. 15, p. 341.

[10]R. Landauer, in *Proceedings of the First Conference on the Electrical and Optical Properties of Inhomogeneous Media,* edited by J. C. Garland and D. B. Tanner, AIP Conference Proceedings No. 40 (American Institute of Physics, New York, 1978), p. 2.

[11]T. W. Noh, A. J. Sievers, L. A. Xue, and R. Raj, Opt. Lett. (to be published).

[12]D. E. Edwards, in *Handbook of Optical Constants of Solids,* edited by E. D. Palik (Academic, New York, 1985), p. 574.